

Platoon Formation in a Mixed Traffic Environment: A Model-Agnostic Optimal Control Approach

A M Ishtiaque Mahbub, *Student Member, IEEE*, Andreas A. Malikopoulos, *Senior Member, IEEE*

Abstract— Coordination of connected and automated vehicles (CAVs) in mixed traffic environment poses significant challenges due to the presence of human-driven vehicles (HDVs) with stochastic dynamics and driving behavior. In earlier work, we addressed the problem of platoon formation of HDVs led by a CAV using a model-dependent, open-loop controller. In this paper, we develop a comprehensive model-agnostic, multi-objective optimal controller which ensures platoon formation of the trailing HDVs by directly controlling the leading CAV without having explicit knowledge of the HDV dynamics. We provide a detailed exposition of the control framework that uses instantaneous motion information from multiple successive HDVs to enforce safety while achieving the optimization objectives. To demonstrate the efficacy of the proposed control framework, we evaluate its performance using numerical simulation and provide associated sensitivity and robustness analysis.

I. INTRODUCTION

The implementation of an emerging transportation system with connected automated vehicles (CAVs) enables a novel computational framework to better monitor the transportation network conditions and make optimal operating decisions to improve safety and reduce pollution, energy consumption, and travel delays [1]. Recent efforts have reported several optimal control approaches for coordination of CAVs at different traffic scenarios such as on-ramp merging roadways [2], roundabouts [3], [4], speed reduction zones [5], signal-free intersections [6]–[10], and traffic corridors [11]–[13]. These approaches have focused on 100% CAV penetration rates without considering human-driven vehicles (HDVs). However, the existence of having a transportation network with a 100% CAVs is not expected before 2060 [14]. Therefore, the need for a mathematically robust and tractable control framework considering a *mixed traffic environment* consisting of both CAVs and HDVs is essential. To establish an automated transportation system, the presence of HDVs pose significant modeling and control challenges to the CAVs due to the stochastic nature of the human-driving behavior. Some approaches reported in the literature [15] have included car-following models (e.g., [16]–[18]) while others have been based on reinforcement learning [19], [20].

In this paper, our research hypothesis is that, since we cannot control the HDVs directly, we can control the CAVs in a way to force the trailing HDVs to form platoons,

This research was supported by ARPAE’s NEXTCAR program under the award number DE-AR0000796.

The authors are with the Department of Mechanical Engineering, University of Delaware, Newark, DE 19716 USA (emails: mahbub@udel.edu; andreas@udel.edu.)

and thus indirectly control the HDVs. In this context, we focus on the problem of vehicle platoon formation in mixed traffic environment by only controlling the CAVs within the network. Although the problem of platoon formation has been widely studied for 100% CAV penetration [21]–[23], only limited efforts have been reported in the literature for mixed traffic environment. Some of these approaches have adopted adaptive cruise control for the CAVs [24]–[26] to maintain platoon stability.

In earlier work [27], we addressed the problem of platoon formation in a mixed environment by developing an open-loop controller for the CAV that has explicit knowledge of the HDV’s car-following model and does not consider any notion of optimality. In this paper, we extend our previous work by introducing a multi-objective optimal control framework for each CAV within the network subject to its state and control constraints. The optimization objectives are (a) to form a platoon with the trailing HDVs, and (b) to improve its fuel economy while achieving (a). Our proposed control framework is *model-agnostic*, i.e., it does not require the explicit knowledge of the HDVs’ car-following model, and employs a receding horizon controller that uses a *multi-successor communication topology*, i.e., reception of instantaneous motion information from multiple trailing HDVs, to enforce safety while deriving and implementing the optimal control input of the CAV. To the best of our knowledge, such approach has not yet been reported in the literature to date.

The remainder of the paper proceeds as follows. In Section II, we provide the modeling framework of the platoon formation problem in a mixed traffic environment. In Section III, we develop a model-agnostic constrained multi-objective optimal control framework for the CAV that enables the platoon formation operation. In Section IV, we evaluate the performance of the proposed control framework using numerical simulation and validate its effectiveness. Finally, we draw concluding remarks and discuss potential directions for future research in Section V.

II. PROBLEM FORMULATION

We consider a CAV followed by one or multiple HDVs traveling in a single-lane roadway of length $L \in \mathbb{R}^+$. We subdivide the roadway into two distinct zones, namely, a *buffer zone* of length $L_b \in \mathbb{R}^+$ where the HDVs’ state information is estimated, as shown in Fig. 1 (top), and a *control zone* of length $L_c \in \mathbb{R}^+$ such that $L = L_b + L_c$, where the leading CAV is to be controlled to form a platoon with the trailing HDVs, as shown in Fig. 1 (bottom). The

CAV enters and leaves the control zone at times $t^c, t^f \in \mathbb{R}^+$, respectively.

Let $\mathcal{N} = \{1, \dots, N\}$, where $N \in \mathbb{N}$ is the total number of vehicles traveling within the buffer zone, be the set of vehicles considered to form a platoon. Here, the leading vehicle indexed by 1 is the CAV, and the rest of the trailing vehicles in $\mathcal{N} \setminus \{1\}$ are HDVs. We denote the set of the HDVs following the CAV to be $\mathcal{N}_{\text{HDV}} = \{2, \dots, N\} \subset \mathcal{N}$. The objective of the CAV $i \in \mathcal{N}$ is to derive and implement the optimal control input (acceleration/deceleration) such that a platoon formation with the trailing HDVs in \mathcal{N}_{HDV} is completed within the control zone of length L_c .

Since the HDVs do not share their local state information with any external agents, we assume the presence of a *coordinator* that gathers the state information of the trailing HDVs traveling within the buffer zone. The coordinator, which can be loop-detectors or comparable sensory devices, in turn, transmits the HDV state information to the CAV at each time instance $t \in [t^c, t^f]$ using standard vehicle-to-infrastructure communication protocol.

We consider a standard double-integrator model to represent the longitudinal dynamics of each vehicle $i \in \mathcal{N}$ within the network at time $t \in [t^c, t^f]$ as

$$\begin{aligned} \dot{p}_i(t) &= v_i(t), \\ \dot{v}_i(t) &= u_i(t), \end{aligned} \quad (1)$$

where $p_i(t) \in \mathcal{P}_i$, $v_i(t) \in \mathcal{V}_i$ and $u_i(t) \in \mathcal{U}_i$ are the position of the front bumper, speed and control input (acceleration command) of each vehicle $i \in \mathcal{N}$, respectively.

The speed $v_i(t)$ and control input $u_i(t)$ of each vehicle $i \in \mathcal{N}$ at time $t \in [t^c, t^f]$ are subject to the following constraints,

$$\begin{aligned} 0 \leq v_{\min} \leq v_i(t) \leq v_{\max}, \\ u_{\min} \leq u_i(t) \leq u_{\max}, \end{aligned} \quad (2)$$

where v_{\min} and v_{\max} are the minimum and maximum allowable speed of the considered roadway, respectively, and u_{\min} and u_{\max} are the minimum and maximum acceleration of each vehicle $i \in \mathcal{N}$, respectively.

Definition 1. The dynamic following spacing $s_i(t)$ between vehicle i and $(i-1) \in \mathcal{N}$ is

$$s_i(t) = \rho \cdot v_i(t) + s_0, \quad (3)$$

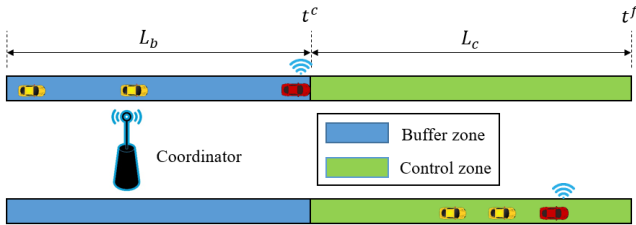


Fig. 1: A CAV (red) traveling with two trailing HDVs (yellow), where the HDVs' state information is estimated (top scenario) by the coordinator within the buffer zone, and the platoon is formed (bottom scenario) by controlling the CAV at the control zone.

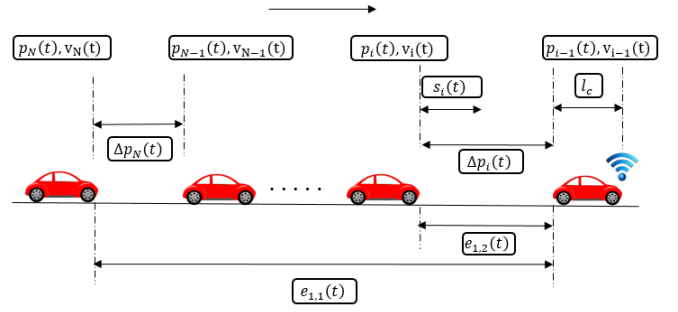


Fig. 2: Predecessor-follower coupled car-following dynamic.

where $\rho \in \mathbb{R}^+$ denotes a desired safety time headway that each HDV $i \in \mathcal{N}_{\text{HDV}}$ maintains while following its preceding vehicle $i-1 \in \mathcal{N}$, and $s_0 \in \mathbb{R}^+$ is the standstill distance denoting the minimum bumper-to-bumper gap at stop.

Definition 2. The *headway* $\Delta p_i(t)$ (Fig. 2) and the *approach rate* $\Delta v_i(t)$ of vehicle $i \in \mathcal{N}$ denote the bumper-to-bumper inter-vehicle spacing and speed difference, respectively, between the two consecutive vehicles $i, (i-1) \in \mathcal{N}$, i.e.,

$$\Delta p_i(t) = p_{i-1}(t) - p_i(t) - l_c, \quad (4)$$

$$\Delta v_i(t) = v_{i-1}(t) - v_i(t), \quad (5)$$

where $l_c \in \mathbb{R}^+$ is the length of each vehicle $i \in \mathcal{N}$.

The rear-end collision avoidance constraint is

$$\Delta p_i(t) \geq s_i(t), \quad \forall t \in [t^c, t^f]. \quad (6)$$

In our modeling framework, we impose the following assumptions.

Assumption 1. For each vehicle $i \in \mathcal{N}$ at time $t = t^c$, none of the state and control constraints in (2) are active.

Assumption 2. No error or delay occurs during the communication between the CAV and the coordinator.

Assumption 1 ensures that the initial state and control input of each vehicle $i \in \mathcal{N}$ are feasible. Assumption 2 may be strong, but it is relatively straightforward to relax as long as the noise in the measurements and/or delays is bounded. For example, we can determine upper bounds on the state uncertainties as a result of sensing or communication errors and delays, and incorporate these into more conservative safety constraints.

The control input $u_i(t)$ of each vehicle $i \in \mathcal{N}$ in (1) can take different forms based on the consideration of connectivity and automation. For CAV $1 \in \mathcal{N}$, we derive and implement the control input $u_1(t)$ using the optimal control framework discussed in Section III. For each HDV $i \in \mathcal{N}_{\text{HDV}}$, however, we consider a car-following model to represent the predecessor-follower coupled dynamics (Fig. 2) which has the following generic structure:

$$u_i(t) = f_{\text{CFM}}(\Delta p_i(t), \Delta v_i(t), v_i(t)), \quad (7)$$

where $f_{\text{CFM}}(\cdot)$ represents the behavioral function of the car-following model.

Remark 1. We restrict the control of the CAV only within the control zone so that we only have a finite optimization horizon $[t^c, t^f]$ to consider. Outside the control zone, the CAV dynamics follows the car-following model in (7).

There are several car-following models reported in the literature [16]–[18], [28] that can emulate a varied class of human driving behavior. Thus, it is unreasonable to restrict the choice of f_{CFM} to a particular car-following model to represent the HDVs. Furthermore, since CAV 1 cannot estimate the driving behavior of the HDVs, in this paper we consider that the behavioral function f_{CFM} of the HDVs is unknown to CAV 1. However, to ensure that any car-following model considered in our modeling framework emulates realistic human driving behavior, we impose the following eligibility criteria.

An eligible car-following model with behavioral function f_{CFM} (see [29] for details) should

(a) obey rational driving behavior, i.e., the following inequalities should hold,

$$\frac{\partial f_{\text{CFM}}}{\partial \Delta p_i(t)} > 0, \quad \frac{\partial f_{\text{CFM}}}{\partial \Delta v_i(t)} > 0, \quad \frac{\partial f_{\text{CFM}}}{\partial v_i(t)} < 0, \quad (8)$$

(b) be platoon stable such that the following characteristic equation parameterized by λ has both negative real part,

$$\lambda^2 + \left(\frac{\partial f_{\text{CFM}}}{\partial \Delta v_i(t)} - \frac{\partial f_{\text{CFM}}}{\partial v_i(t)} \right) \lambda + \frac{\partial f_{\text{CFM}}}{\partial \Delta p_i(t)} = 0, \quad \text{and} \quad (9)$$

(c) be string stable such that the following condition holds

$$\frac{\frac{\partial f_{\text{CFM}}}{\partial \Delta p_i(t)}}{\left(\frac{\partial f_{\text{CFM}}}{\partial v_i(t)} \right)^3} \left[\frac{\left(\frac{\partial f_{\text{CFM}}}{\partial v_i(t)} \right)^2}{2} - \frac{\partial f_{\text{CFM}}}{\partial v_i(t)} \cdot \frac{\partial f_{\text{CFM}}}{\partial \Delta v_i(t)} - \frac{\partial f_{\text{CFM}}}{\partial \Delta p_i(t)} \right] < 0. \quad (10)$$

Next, we provide some definitions that are necessary in our exposition.

Definition 3. The information set $\mathcal{I}_1(t)$ of CAV $1 \in \mathcal{N}$ at time $t \in [t^c, t^f]$ is

$$\mathcal{I}_1(t) = \{p_{1:N}(t), v_{1:N}(t)\}, \quad (11)$$

where $p_{1:N}(t) = [p_1(t), \dots, p_N(t)]^T$ and $v_{1:N}(t) = [v_1(t), \dots, v_N(t)]^T$.

Definition 4. A platoon formation is established at some time $t^p \in (t^c, t^f)$ if for each vehicle $i \in \mathcal{N}$, the headway $\Delta p_i(t)$ converges to an equilibrium headway Δp_{eq} , and the approach rate $\Delta v_i(t)$ converges to zero, i.e.,

$$\Delta p_i(t) = \Delta p_{eq}, \quad \Delta p_{eq} \in \mathbb{R}^+, \quad \forall t \geq t^p, \quad (12)$$

$$\Delta v_i(t) = 0, \quad \forall t \geq t^p, \quad (13)$$

Note that, when the approach rate $\Delta v_i(t)$ converges to zero, the speed $v_i(t)$ of each vehicle $i \in \mathcal{N}$ also converges to an equilibrium platoon speed v_{eq} .

Remark 2. In real-world applications, conditions (12)–(13) might be too restrictive to establish a platoon formation. Therefore, we relax these conditions and introduce

the following root-mean-squared error-based conditions to establish a platoon formation at some time $t^p \in (t^c, t^f)$,

$$\sqrt{\frac{1}{N-1} \sum_{i=2}^N (\Delta p_i(t) - \mu_{\Delta p}(t))^2} \leq \epsilon_{\Delta p}, \quad \forall t \geq t^p, \quad (14)$$

$$\sqrt{\frac{1}{N} \sum_{i=1}^N (v_i(t) - \mu_v(t))^2} \leq \epsilon_v, \quad \forall t \geq t^p, \quad (15)$$

where $\mu_{\Delta p}(t) := \frac{\sum_{i=2}^N \Delta p_i(t)}{N}$ and $\mu_v(t) := \frac{\sum_{i=1}^N v_i(t)}{N}$ are the mean headway and mean speed of N vehicles, respectively, and $\epsilon_{\Delta p}$ and ϵ_v are the allowable deviation of $\Delta p_i(t)$ and $v_i(t)$ from the equilibrium values Δp_{eq} and v_{eq} , respectively. The conditions in (14) and (15) mean that a platoon formation is established at time $t = t^p$ when the root-mean-squared errors of the headway $\Delta p_i(t)$ and speed $v_i(t)$ for all $i \in \mathcal{N}$ at time $t \geq t^p$ become less or equal to the allowable deviations $\epsilon_{\Delta p}$ and ϵ_v , respectively.

Next, we formally state the platoon formation problem in mixed environment as follows.

Problem 1. Given the information set $\mathcal{I}_1(t)$ at time $t = t^c$, the objective of the CAV $1 \in \mathcal{N}$ is to derive its optimal control input $u_1^*(t)$ so that the each vehicle $i \in \mathcal{N}$ achieves a platoon formation (Definition 4) within the control zone.

Remark 3. In our framework, CAV 1 derives its optimal control input $u_1^*(t)$ by solving an optimal control problem with the following objectives: (a) formation of platoon with the trailing HDVs (Definition 4), and (b) improvement of its fuel economy while achieving (a).

In this paper, we adopt a receding horizon control framework with multi-successor communication topology to address Problem 1. In what follows, we provide a detailed exposition of the receding horizon control framework that leads to an optimal platoon formation (Remark 3).

III. RECEDING HORIZON CONTROL

The basic principle of a receding horizon control is that, the optimal control input sequence at current time instance is obtained by solving online an optimal control problem with the prediction horizon T_p , and only the first element of the solved optimal control input sequence is implemented. Afterwards, the horizon moves forward one step, and the above process is repeated until the optimization horizon T_h is reached.

Remark 4. In our problem formulation, the exit time t^f of the CAV 1 from the control zone depends on the nature of the optimal control input of CAV 1, and thus, it is not known a priori. Let t^e be the time that the CAV exits the control zone when cruising with a constant speed inside the control zone. Then, $t^e = t^c + \frac{L_c}{v_1(t^c)}$. In our previous work [27], we have shown that a platoon formation with trailing HDVs can be achieved by non-positive control trajectory of the CAV. Consequently, if we aim at forming the platoon by considering the optimization horizon to be $T_h = t^e - t^c$,

then we need to ensure that the platoon is formed within the control zone.

In this paper, for the CAV, we use a receding horizon to achieve the optimization objectives outlined in Remark 3 while enforcing rear-end collision avoidance constraint with its trailing HDV. To this end, the adoption of the CAV dynamics in (1) is not sufficient; our proposed control framework requires the consideration of an augmented CAV dynamics.

A. Augmented CAV dynamics

To capture the additional characteristics of the platoon formation dynamics from the CAV's control point of view, our proposed control framework uses instantaneous motion information from multiple successive HDVs. Hence, we define two additional states as follows.

Definition 5. The *head-to-tail gap* of the platoon, $e_{1,1}(t)$, is the bumper-to-bumper gap between the CAV and the last trailing HDV $N \in \mathcal{N}$ of the desired platoon, and the *leader-follower gap*, $e_{1,2}(t)$, is the bumper-to-bumper gap between the CAV and the immediately trailing HDV $2 \in \mathcal{N}$ (Fig. 2). Therefore, we have

$$e_{1,1}(t) = p_1(t) - p_N(t) - (N - 1)l_c, \quad (16)$$

$$e_{1,2}(t) = p_1(t) - p_2(t) - l_c. \quad (17)$$

The additional states $e_{1,1}(t)$ and $e_{1,2}(t)$ enables the augmentation of the CAV dynamics (1) with the following set of equations,

$$\dot{e}_{1,1}(t) = v_1(t) - v_N(t), \quad (18)$$

$$\dot{e}_{1,2}(t) = v_1(t) - v_2(t). \quad (19)$$

Remark 5. The consideration of the head-to-tail gap $e_{1,1}(t)$ of the platoon enables the formulation of the objective function for the platoon formation problem whereas the leader-follower gap $e_{1,2}(t)$ enables the enforcement of rear-end collision avoidance constraint in (6), leading to a safe platoon formation.

B. Discrete Time Formulation

To enable the application of discrete receding horizon control, we need to formulate the optimal control problem in discrete time. Suppose, the optimization horizon T_h is discretized by a sampling time interval τ leading to discrete time instance k . Assuming constant value of control input $u_1(k)$ during each time step $[k, (k + 1)]$, we recast the augmented CAV dynamics (1) and (18)-(19) as linear discrete-time state equations

$$p_1(k + 1) = p_1(k) + v_1(k)\tau + \frac{1}{2}u_1(k)\tau^2, \quad (20)$$

$$v_1(k + 1) = v_1(k) + u_1(k)\tau, \quad (21)$$

$$e_{1,1}(k + 1) = e_{1,1}(k) + (v_1(k) - v_N(k))\tau + \frac{1}{2}u_1\tau^2, \quad (22)$$

$$e_{1,2}(k + 1) = e_{1,2}(k) + (v_1(k) - v_2(k))\tau + \frac{1}{2}u_1\tau^2. \quad (23)$$

We define the current state vector $x_1(k)$, measured output vector $y_1(k)$ and the measured disturbance vector $w_1(k)$ as

$$x_1(k) := \begin{bmatrix} p_1(k) \\ v_1(k) \\ e_{1,1}(k) \\ e_{1,2}(k) \end{bmatrix}, y_1(k) := \begin{bmatrix} v_1(k) \\ e_{1,1}(k) \\ e_{1,2}(k) \end{bmatrix}, w_1(k) := \begin{bmatrix} v_N(k) \\ v_2(k) \end{bmatrix}.$$

The state-space representation of the discrete dynamic in (20)-(23) is thus

$$x_1(k + 1) = Ax_1(k) + B_u u_1(k) + B_w w_1(k), \quad (24)$$

$$y_1(k) = Cx_1(k), \quad (25)$$

where, the corresponding state matrix A , control matrix B_u , disturbance matrix B_w and output matrix C can be computed as

$$A = \begin{bmatrix} 1 & \tau & 0 & 0 \\ 0 & 1 & 0 & 0 \\ 0 & \tau & 1 & 0 \\ 0 & \tau & 0 & 1 \end{bmatrix}, B_u = \begin{bmatrix} \frac{1}{2}\tau^2 \\ \tau \\ \frac{1}{2}\tau^2 \\ \frac{1}{2}\tau^2 \end{bmatrix},$$

$$B_w = \begin{bmatrix} 0 & 0 \\ 0 & 0 \\ -\tau & 0 \\ 0 & -\tau \end{bmatrix}, C = \begin{bmatrix} 0 & 1 & 0 & 0 \\ 0 & 0 & 1 & 0 \\ 0 & 0 & 0 & 1 \end{bmatrix}.$$

For the remainder of this paper, we drop the subscript 1 denoting the CAV from the discrete state-space model where it does not introduce ambiguity.

C. Prediction Model

In order to solve an online optimization within the prediction horizon T_p , the receding horizon controller requires a prediction model to take into account the future possible states. In general, the future system states are predicted based on the model (24)-(25) and the current state information $x(k)$. Let us denote the predicted state, predicted output, control and disturbance vector given the prediction horizon T_p and control horizon T_c to be $\tilde{X}(k + T_p|k)$, $\tilde{Y}(k + T_p|k)$, $U(k + T_c)$ and $W(k + T_p)$, respectively, which has the following structure

$$\tilde{X}(k + T_p|k) = \begin{bmatrix} \tilde{x}(k + 1|k) \\ \tilde{x}(k + 2|k) \\ \vdots \\ \tilde{x}(k + T_p|k) \end{bmatrix}, U(k + T_c) = \begin{bmatrix} u(k) \\ u(k + 1) \\ \vdots \\ u(k + T_c - 1) \end{bmatrix},$$

$$\tilde{Y}(k + T_p|k) = \begin{bmatrix} \tilde{y}(k + 1|k) \\ \tilde{y}(k + 2|k) \\ \vdots \\ \tilde{y}(k + T_p|k) \end{bmatrix}, W(k + T_p) = \begin{bmatrix} w(k) \\ w(k + 1) \\ \vdots \\ w(k + T_p - 1) \end{bmatrix},$$

where $\tilde{x}(k + n|k)$, $\tilde{y}(k + n|k)$, and $w(k + n - 1)$, $n = 1, \dots, T_p$, denote the predicted state, output and disturbance values, respectively, within the prediction horizon T_p based on their value at the discrete instance k . Note that, the optimal control sequence $u^*(k + m - 1)$, $m = 1, \dots, T_c$ are to be determined by solving the open-loop optimal control problem for the prediction horizon T_p .

The predictive state and associated performance vectors of the receding horizon controller can subsequently be represented as

$$\tilde{X}(k + T_p|k) = \tilde{A}x(k) + \tilde{B}_u U(k + T_c) + \tilde{B}_d W(k + T_p), \quad (26)$$

$$\tilde{Y}(k + T_p|k) = \tilde{C}x(k) + \tilde{D}_u U(k + T_c) + \tilde{D}_d W(k + T_p), \quad (27)$$

where the predictive system matrices \tilde{A} , \tilde{B}_u , \tilde{B}_d , \tilde{C} and \tilde{D} can be computed as

$$\begin{aligned}\tilde{A} &= [A \quad A^2 \quad \cdots \quad A^{T_p}]^T, \\ \tilde{B}_u &= \begin{bmatrix} B_u & 0 & \cdots & 0 \\ AB_u & B_u & \cdots & 0 \\ \vdots & \vdots & \ddots & \vdots \\ A^{T_p-1}B_u & A^{T_p-2}B_u & \cdots & A^{T_p-T_c}B_u \end{bmatrix}, \\ \tilde{B}_d &= \begin{bmatrix} B_d & 0 & \cdots & 0 \\ AB_d & B_d & \cdots & 0 \\ \vdots & \vdots & \ddots & \vdots \\ A^{T_p-1}B_d & A^{T_p-2}B_d & \cdots & B_d \end{bmatrix}, \tilde{C} = \begin{bmatrix} CA \\ CA^2 \\ \vdots \\ CA^{T_p} \end{bmatrix}, \\ \tilde{D}_u &= \begin{bmatrix} CB_u & 0 & \cdots & 0 \\ CAB_u & CB_u & \cdots & 0 \\ \vdots & \vdots & \ddots & \vdots \\ CA^{T_p-1}B_u & CA^{T_p-2}B_u & \cdots & CA^{T_p-T_c}B_u \end{bmatrix}, \\ \tilde{D}_d &= \begin{bmatrix} CB_d & 0 & \cdots & 0 \\ CAB_d & CB_d & \cdots & 0 \\ \vdots & \vdots & \ddots & \vdots \\ CA^{T_p-1}B_d & CA^{T_p-2}B_d & \cdots & CB_d \end{bmatrix}.\end{aligned}$$

In our formulation, we consider that the measured disturbance $w(k)$ in (26)-(27) remains constant within the prediction horizon T_p . Therefore, we have

$$w(k+n|k) = w(k), \quad n = 1, \dots, T_p. \quad (28)$$

Consequently, the disturbance vector can be computed as $W(k+T_p) = [w(k), \dots, w(k)]^T$. The inaccuracy in modeling the predicted disturbance vector $W(k+T_p)$ can be compensated by incorporating a feedback scheme into the receding horizon optimization [30].

D. Objective Functions

Let us define $\|z\|_M$ to be the M weighted norm of an arbitrary vector z such that $\|z\|_M := (z^T M z)^{\frac{1}{2}}$. In order to drive each HDV's state towards the equilibrium platoon state, the primary aim of the CAV controller is to minimize the squared error between the predicted output $\tilde{y}(k+n|k)$, $n = 1, 2, \dots, T_p$, and the corresponding reference output. The first objective function thus represents a reference tracking problem and takes the form

$$J_1 := \frac{1}{2} \sum_{n=1}^{T_p} \|\tilde{y}(k+n|k) - y_r(k+n)\|_{\bar{Q}}^2, \quad (29)$$

where the reference output $y_r(k)$ and the output weight matrix \bar{Q} are defined as

$$\begin{aligned}y_r(k) &:= (N-1)(s_0 + \rho [1 \quad 0] w(k)), \quad (30) \\ \bar{Q} &:= \begin{bmatrix} q_v & 0 & 0 \\ 0 & q_{e_1} & 0 \\ 0 & 0 & q_{e_2} \end{bmatrix},\end{aligned}$$

with the diagonal weight parameters q_v , q_{e_1} , q_{e_2} corresponding to the speed $v_1(k)$, head-to-tail gap $e_{1,1}(k)$ and leader-follower gap $e_{1,2}(k)$, respectively. In order to keep

the output error term small and error squared non-negative, \bar{Q} must be positive semidefinite, i.e., $\bar{Q} = \bar{Q}^T \geq 0$. Since the measured disturbance $w(k)$ remains constant within the prediction horizon T_p (28), and the reference output $y_r(k)$ is an explicit function of the measured disturbance $w(k)$ (30), the predictive reference output $y_r(k+n|k)$, $n = 1, \dots, T_p$ remains constant within the prediction horizon T_p as well. Thus we have

$$y_r(k+n|k) = y_r(k), \quad n = 1, \dots, T_p. \quad (31)$$

The second objective of the controller is to improve the fuel economy of the CAV by minimizing its transient engine behavior. Therefore, we minimize the L^2 -norm of the CAV's control input by defining the following objective function

$$J_2 := \frac{1}{2} \sum_{m=1}^{N_c} \|u(k+m-1)\|_R^2, \quad (32)$$

where $R := [w_r]$ is the weight matrix on the control input with weight parameter w_r . The cost of the control input has to be a positive quantity, thus the matrix R should be positive definite. This leads to $R = R^T > 0$ which implies $w_r > 0$.

Finally, combining the objective functions defined in (29) and (32), and using the compact notations from (26)-(27), we have the final objective function as follows

$$J = \frac{1}{2} \|\tilde{Y}(k+T_p|k) - Y_r\|_{\bar{Q}}^2 + \frac{1}{2} \|U(k+T_c)\|_{\bar{R}}^2, \quad (33)$$

where

$$\begin{aligned}Y_r &= [y_r(k) \cdots y_r(k)]^T \\ &= (N-1) \left(s_0 \begin{bmatrix} 1 \\ \vdots \\ 1 \end{bmatrix} + \rho \begin{bmatrix} 1 & 0 \\ \vdots & \vdots \\ 1 & 0 \end{bmatrix} w(k) \right), \text{ and} \\ \bar{Q} &= \begin{bmatrix} Q & \cdots & 0 \\ \vdots & \ddots & \vdots \\ 0 & \cdots & Q \end{bmatrix}, \quad \bar{R} = \begin{bmatrix} R & \cdots & 0 \\ \vdots & \ddots & \vdots \\ 0 & \cdots & R \end{bmatrix}.\end{aligned}$$

E. Constraints

In standard receding horizon formulation, constraints are classified as either hard or soft [31]. Hard constraints must always be satisfied where any violation may lead to infeasible solution of the optimal control problem. On the other hand, soft constraints may be violated if necessary to avoid such infeasible solution. Hence, limited number of hard constraints are desired. In our formulation, we consider the control input constraints in (2) and the safety constraint in (6) to be hard due to the physical limitation of the CAV dynamics and passenger safety, respectively. On the other hand, we consider the speed constraints in (2) to be soft. However, significantly large penalty is incorporated into the objective function J in (33) using a dimensionless, non-negative slack variable to handle the soft constraint violation, the exposition of which is outside the scope of this paper. The constraints in the context of the receding horizon control framework are

thus given as

Hard Constraints:

$$u_{\min} \leq u(k+m-1) \leq u_{\max}, \quad m = 1, \dots, T_c,$$

$$e_{1,1}(k+n) \geq (N-1)s_0, \quad n = 1, \dots, T_p,$$

$$e_{1,2}(k+n) \geq s_0, \quad n = 1, \dots, T_p,$$

Soft Constraint:

$$v_{\min} \leq v(k+n) \leq v_{\max}, \quad n = 1, \dots, T_p. \quad (34)$$

F. The Optimal Control Problem

With the objective function (33), constraints (34), dynamics model (20)-(23), and the information set $\mathcal{I}_1(k)$, $k = 0, \dots, T_h$ at hand, the optimal control problem can finally be written as

$$\min_{U(k+T_c)} J, \quad (35)$$

subject to :

model: (20) – (23), constraints: (34),

and given $\mathcal{I}_1(k)$.

The optimal control problem in (35) can be transformed into a standard constrained quadratic programming problem and solved using commercially available solvers [30]. At each discrete time k , the CAV measures the information set $\mathcal{I}_1(k)$. Using these measurements, the optimal control sequence $U^*(k+T_c)$ is computed by solving (35) and only the first control input $u^*(k)$ is applied. Then the system moves to the next time instance $k+1$ and the process is repeated until T_h is reached.

IV. SIMULATION RESULTS

To evaluate the performance of the proposed control framework, we adopt two widely applied car-following models, namely, the optimal velocity model (OVM) [28] and the intelligent driver model (IDM) [18], to represent the predecessor-follower coupled dynamics (Fig. 2) of each HDV $i \in \mathcal{N}_{\text{HDV}}$. Our decision for choosing the OVM and IDM car-following model stems from the fact that (a) they implement explicit and implicit equilibrium speed-headway function, respectively, presenting our proposed model-agnostic control framework with broader challenge, and (b) both of these models satisfy the eligibility conditions in (8)-(10) [29]. One of the simplest forms of the OVM car-following model [28] is given as

$$u_i(t) = \alpha(V_i(\delta_i(t), s_i(t)) - v_i(t)), \quad (36)$$

$$V_i(\delta_i(t), s_i(t)) = \frac{v_d}{2} (\tanh(\delta_i(t)) + \tanh(s_i(t))),$$

where $\delta_i(t) := \Delta p_i(t) - s_i(t)$, and α , $V_i(\delta_i(t), s_i(t))$ and v_d denote the control gain representing the driver's sensitivity coefficient, the equilibrium speed-headway function and the desired speed of the roadway, respectively. The IDM car-following model [18] for HDV $i \in \mathcal{N}_{\text{HDV}}$ has the following

structure

$$u_i(t) = a \left(1 - \left(\frac{v_i(t)}{v_d} \right)^\gamma - \left(\frac{\Delta \bar{p}_i(t)}{\Delta p_i(t)} \right)^2 \right), \quad (37)$$

$$\Delta \bar{p}_i(t) = s_i(t) + \frac{v_i(t) \Delta v_i(t)}{2ab},$$

where, a , b and γ are the desired acceleration, comfortable braking and acceleration exponent, respectively. The car-following model and receding horizon controller parameters considered in our numerical study are given in Tables I and II, respectively.

TABLE I: Simulation parameters considered.

Parameters	Values
Minimum speed, v_{\min}	10.0 [m/s]
Maximum speed, v_{\max}	30.0 [m/s]
Maximum deceleration, u_{\min}	-3.0 [m/s ²]
Maximum acceleration, u_{\max}	2.0 [m/s ²]
Safe time headway, ρ	1.5 [s]
Vehicle length, l_c	5 [m]
Buffer zone length, L_b	500 [m]
Control zone length, L_c	1500 [m]
Optimal velocity model (36)	
Driver's sensitivity coefficient, α	1.0
Desired speed, v_d	30.0 [m/s]
Intelligent driver model (37)	
Acceleration exponent, γ	4.0
Comfortable braking, b	3.0 [m/s ²]
Desired acceleration, a	2.0 [m/s ²]

TABLE II: Receding horizon controller parameters

Parameters	Values
Optimization horizon, T_h	65.0 [s]
Prediction horizon, T_p	10.0 [s]
Control horizon, T_c	2.0 [s]
Sample time, τ	0.1 [s]
Input weight, w_r	5.0
Output weight, Q	diag(0.2, 0, 0)

We conduct the simulation studies using MATLAB R2020b/Simulink with the configuration of Intel Core i7-6700 CPU @ 3.40 GHz. For the first case study, a platoon formation for $N = 4$ vehicles is shown Fig. 3, where the OVM model in (36) is considered for the trailing HDVs. The leading CAV and trailing HDVs have randomly selected initial position (Fig. 3(a)) and initial speed (Fig. 3(c)), respectively. The lead CAV implements our proposed controller to complete the platoon formation operation near 50 s (according to Remark 2), and the vehicle headway (Fig. 3(b)) and speed (Fig. 3(c)) converges to an equilibrium value. Additionally, none of the control, safety, and speed constraints in (34) were violated during the platoon formation as evident from the headway profile in Fig. 3(b), speed profile in 3(c), and CAV's control input trajectory in Fig. 3(d), respectively. To verify that the proposed control framework is indeed model-agnostic, we present a second case study (see Fig. 4) for $N = 4$ with similar initial conditions as in the previous case (see Fig. 3), but implementing the IDM model (37) for the HDVs instead. Platoon formation was achieved within the given optimization horizon T_h without violating

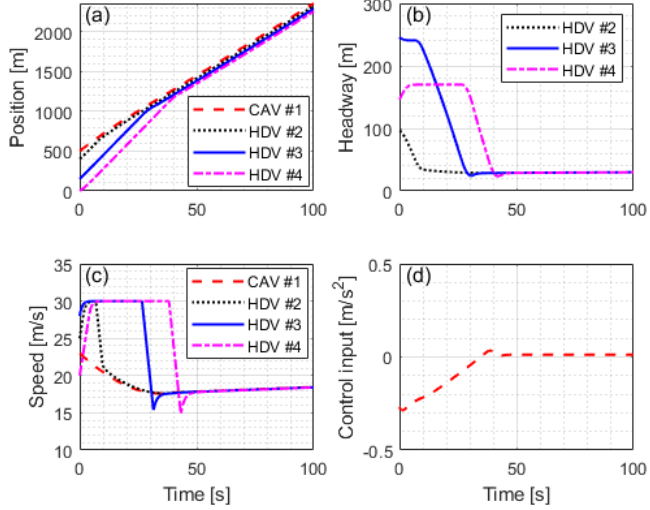


Fig. 3: Platoon formation with OVM car-following model (36) for $N = 4$, where the (a) position trajectory, (b) vehicle headway, (c) speed trajectory and (d) the CAV control trajectory are shown.

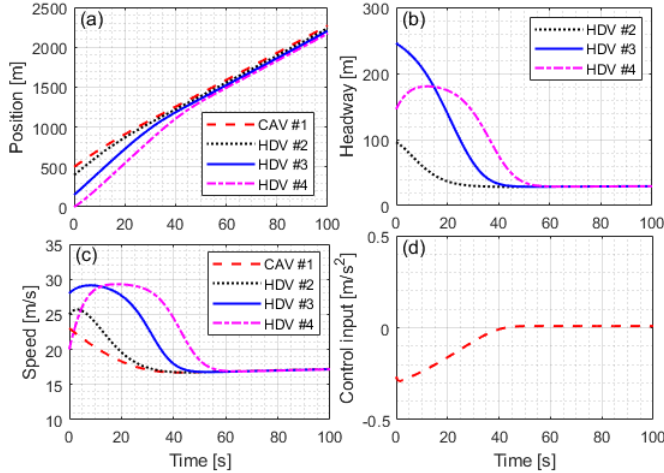


Fig. 4: Platoon formation with IDM car-following model (37) for $N = 4$, where the (a) position trajectory and (b) vehicle headway, (c) speed trajectory and (d) the CAV control trajectory are shown.

any of the control, safety, and speed constraints in (34), as shown in Fig. 4(a)-(d). It is interesting to note that, we have monotonically increasing non-positive linear optimal control input trajectory of the CAV while forming the platoon in both of the above cases (see Figs. 3(d) and 4(d)), which resemble the typical energy-optimal control input trajectory derived using standard Hamiltonian analysis [10], [32].

Figure 5 shows the sensitivity analysis of the proposed control framework for $N = 4$ subject to varying controller parameters T_p, T_c , and τ , and IDM car-following parameter ρ . Note that, the platoon formation time is computed with (14) and (15) presented in Remark 2. Increasing the pre-

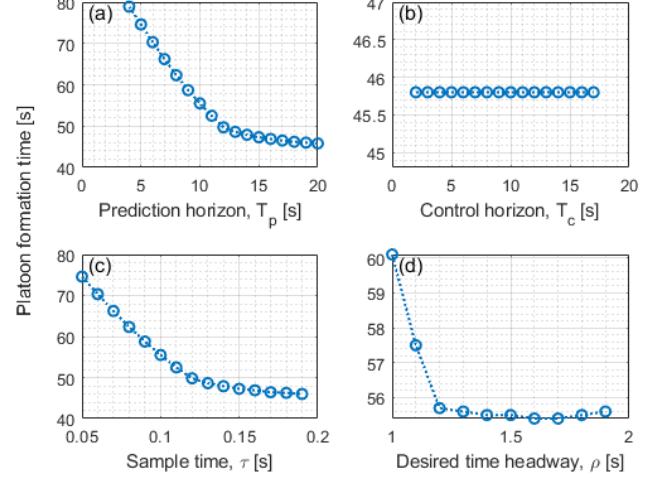


Fig. 5: Platoon formation with IDM car-following model (37) for $N = 4$, where the sensitivity of the platoon formation time under varying (a) prediction horizon T_p , (b) control horizon T_c , (c) sample time τ and (d) desired time headway ρ are illustrated.

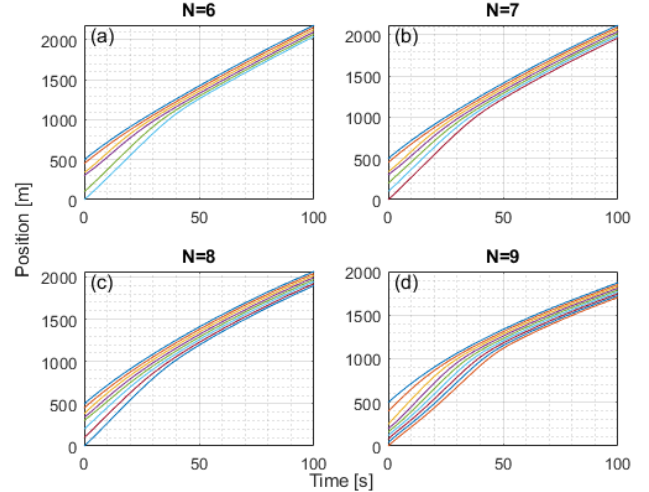


Fig. 6: Safe platoon formation with IDM car-following model (37) for 6, 7, 8 and 9 vehicles.

diction horizon T_p and sample time τ decrease the platoon formation time, as shown in Figs. 5(a) and 5(c), respectively. In contrast, the variation of the control horizon T_c does not affect the platoon formation time, as shown in Fig. 5(b). However, choosing appropriate T_c is essential to enforce the constraints in (34). The platoon formation time under varying desired time headway ρ , which indicates different driving behavior of the IDM car-following model, is shown in Fig. 5(d), which indicates that our proposed framework is robust enough to form a platoon within the desired optimization horizon T_h . In all of the cases presented in Figs. 5(a)-(d), the proposed controller enables platoon formation without violating any constraints in (34). Note that, the parameters

T_p and τ can be tuned using Figs. 5(a) and 5(c) to form a platoon within the desired optimization horizon.

Finally, we investigate the robustness of the proposed framework under different platoon size $N = 6, 7, 8$ and 9 as shown in Fig. 6. The position trajectories of the vehicles in Fig. 6 indicates that the CAV controller is able to form platoon within the designated optimization horizon $T_h = 65$ s without violating any rear-end collision avoidance constraint in (6).

V. DISCUSSION AND CONCLUDING REMARKS

In this paper, we presented a constrained multi-objective optimal control framework for platoon formation under a mixed traffic environment, where a leading CAV computes and implements its optimal control input to force the following HDVs to form a platoon. We developed a model-agnostic receding horizon control framework with a multi-successor communication topology that solves in real time the optimal control problem and provided detailed sensitivity and robustness analysis using numerical simulation to validate the performance of the proposed framework.

A direction for future research should extend the proposed framework for optimal coordination of mixed vehicle platoon in traffic scenarios such as on-ramp merging, urban intersection, etc. Ongoing research investigates the incorporation of non-linear state-space representation and different communication topology to improve the controller performance.

REFERENCES

- [1] J. Guanetti, Y. Kim, and F. Borrelli, "Control of Connected and Automated Vehicles: State of the Art and Future Challenges," *Annual Reviews in Control*, vol. 45, pp. 18–40, 2018.
- [2] I. A. Ntousakis, I. K. Nikolos, and M. Papageorgiou, "Optimal vehicle trajectory planning in the context of cooperative merging on highways," *Transportation Research Part C: Emerging Technologies*, vol. 71, pp. 464–488, 2016.
- [3] L. Zhao, A. A. Malikopoulos, and J. Rios-Torres, "Optimal control of connected and automated vehicles at roundabouts: An investigation in a mixed-traffic environment," in *15th IFAC Symposium on Control in Transportation Systems*, 2018, pp. 73–78.
- [4] A. Bakibillah, M. Kamal, C. Tan *et al.*, "The optimal coordination of connected and automated vehicles at roundabouts," in *2019 58th Annual Conference of the Society of Instrument and Control Engineers of Japan (SICE)*. IEEE, 2019, pp. 1392–1397.
- [5] A. A. Malikopoulos, S. Hong, B. Park, J. Lee, and S. Ryu, "Optimal control for speed harmonization of automated vehicles," *IEEE Transactions on Intelligent Transportation Systems*, vol. 20, no. 7, pp. 2405–2417, 2019.
- [6] A. Colombo and D. Del Vecchio, "Least Restrictive Supervisors for Intersection Collision Avoidance: A Scheduling Approach," *IEEE Transactions on Automatic Control*, vol. Provisiona, 2014.
- [7] K.-D. Kim and P. Kumar, "An MPC-Based Approach to Provable System-Wide Safety and Liveness of Autonomous Ground Traffic," *IEEE Transactions on Automatic Control*, vol. 59, no. 12, pp. 3341–3356, 2014.
- [8] T.-C. Au, S. Zhang, and P. Stone, "Autonomous intersection management for semi-autonomous vehicles," *Handbook of Transportation, Routledge, Taylor & Francis Group.*, 2015.
- [9] A. M. I. Mahbub, L. Zhao, D. Assanis, and A. A. Malikopoulos, "Energy-Optimal Coordination of Connected and Automated Vehicles at Multiple Intersections," in *Proceedings of 2019 American Control Conference*, 2019, pp. 2664–2669.
- [10] A. A. Malikopoulos, L. E. Beaver, and I. V. Chremos, "Optimal time trajectory and coordination for connected and automated vehicles," *Automatica*, vol. 125, no. 109469, 2021.
- [11] J. Lee, B. B. Park, K. Malakorn, and J. J. So, "Sustainability assessments of cooperative vehicle intersection control at an urban corridor," *Transportation Research Part C: Emerging Technologies*, vol. 32, pp. 193–206, 2013.
- [12] A. I. Mahbub, A. A. Malikopoulos, and L. Zhao, "Decentralized optimal coordination of connected and automated vehicles for multiple traffic scenarios," *Automatica*, vol. 117, no. 108958, 2020.
- [13] L. E. Beaver, B. Chalaki, A. M. Mahbub, L. Zhao, R. Zayas, and A. A. Malikopoulos, "Demonstration of a Time-Efficient Mobility System Using a Scaled Smart City," *Vehicle System Dynamics*, vol. 58, no. 5, pp. 787–804, 2020.
- [14] A. Alessandrini, A. Campagna, P. Delle Site, F. Filippi, and L. Persia, "Automated vehicles and the rethinking of mobility and cities," *Transportation Research Procedia*, vol. 5, pp. 145–160, 2015.
- [15] N. Wan, A. Vahidi, and A. Luckow, "Optimal speed advisory for connected vehicles in arterial roads and the impact on mixed traffic," *Transportation Research Part C: Emerging Technologies*, vol. 69, pp. 548–563, 2016.
- [16] P. Gipps, "A behavioural car-following model for computer simulation," *Transportation Research Part B: Methodological*, vol. 15, no. 2, pp. 105–111, 1981.
- [17] R. Wiedemann, "Simulation des strassenverkehrsflusses." 1974.
- [18] M. Treiber and A. Kesting, "Traffic flow dynamics," *Traffic Flow Dynamics: Data, Models and Simulation, Springer-Verlag Berlin Heidelberg*, 2013.
- [19] A. R. Kreidieh, C. Wu, and A. M. Bayen, "Dissipating stop-and-go waves in closed and open networks via deep reinforcement learning," in *2018 21st International Conference on Intelligent Transportation Systems (ITSC)*. IEEE, 2018, pp. 1475–1480.
- [20] C. Wu, K. Parvate, N. Kheterpal, L. Dickstein, A. Mehta, E. Vinitzky, and A. M. Bayen, "Framework for control and deep reinforcement learning in traffic," in *2017 IEEE 20th International Conference on Intelligent Transportation Systems (ITSC)*. IEEE, 2017, pp. 1–8.
- [21] Y. Zheng, S. E. Li, K. Li, and W. Ren, "Platooning of connected vehicles with undirected topologies: Robustness analysis and distributed h-infinity controller synthesis," *IEEE Transactions on Intelligent Transportation Systems*, vol. 19, no. 5, pp. 1353–1364, 2017.
- [22] W. B. Dunbar and R. M. Murray, "Distributed receding horizon control for multi-vehicle formation stabilization," *Automatica*, vol. 42, no. 4, pp. 549–558, 2006.
- [23] G. Orosz, "Connected cruise control: modelling, delay effects, and nonlinear behaviour," *Vehicle System Dynamics*, vol. 54, no. 8, pp. 1147–1176, 2016.
- [24] I. G. Jin, G. Orosz, D. Hajdu, T. Insperger, and J. Moehlis, "To delay or not to delay—stability of connected cruise control," in *Time Delay Systems*. Springer, 2017, pp. 263–282.
- [25] D. Hajdu, I. G. Jin, T. Insperger, and G. Orosz, "Robust design of connected cruise control among human-driven vehicles," *IEEE Transactions on Intelligent Transportation Systems*, vol. 21, no. 2, pp. 749–761, 2019.
- [26] R. A. Dollar, T. G. Molnár, A. Vahidi, and G. Orosz, "Mpc-based connected cruise control with multiple human predecessors," in *2021 American Control Conference (ACC)*. IEEE, 2021, pp. 405–411.
- [27] A. M. I. Mahbub and A. A. Malikopoulos, "A Platoon Formation Framework in a Mixed Traffic Environment," *IEEE Control Systems Letters (LCCS)*, vol. 6, pp. 1370–1375, 2021.
- [28] M. Bando, K. Hasebe, A. Nakayama, A. Shibata, and Y. Sugiyama, "Dynamical model of traffic congestion and numerical simulation," *Physical review E*, vol. 51, no. 2, p. 1035, 1995.
- [29] R. E. Wilson and J. A. Ward, "Car-following models: fifty years of linear stability analysis—a mathematical perspective," *Transportation Planning and Technology*, vol. 34, no. 1, pp. 3–18, 2011.
- [30] F. Borrelli, A. Bemporad, and M. Morari, *Predictive control for linear and hybrid systems*. Cambridge University Press, 2017.
- [31] L.-h. Luo, H. Liu, P. Li, and H. Wang, "Model predictive control for adaptive cruise control with multi-objectives: comfort, fuel-economy, safety and car-following," *Journal of Zhejiang University SCIENCE A*, vol. 11, no. 3, pp. 191–201, 2010.
- [32] A. M. I. Mahbub and A. A. Malikopoulos, "Conditions to Provable System-Wide Optimal Coordination of Connected and Automated Vehicles," *Automatica*, vol. 131, no. 109751, 2021.